Neurobiology of Disease

The Bed Nucleus of the Stria Terminalis Is Critical for Anxiety-Related Behavior Evoked by CO_2 and Acidosis

Rebecca J. Taugher,[1,2] Yuan Lu,[2] Yimo Wang,[2] Collin J. Kreple,[3,4] Ali Ghobbeh,[2] Rong Fan,[2] Levi P. Sowers,[5] and John A. Wemmie[1,2,3,4,6,7]

[1]Interdisciplinary Graduate Program in Neuroscience, University of Iowa, Iowa City, Iowa 52242, [2]Department of Psychiatry, University of Iowa, Iowa City, Iowa 52242, [3]Medical Scientist Training Program, University of Iowa, Iowa City, Iowa 52242, [4]Department of Molecular Physiology and Biophysics, University of Iowa, Iowa City, Iowa 52242, [5]Department of Neurology, University of Iowa, Iowa City, Iowa 52242, [6]Department of Neurosurgery, University of Iowa, Iowa City, Iowa 52242, and [7]Department of Veterans Affairs Medical Center, Iowa City, Iowa 52246

Carbon dioxide (CO_2) inhalation lowers brain pH and induces anxiety, fear, and panic responses in humans. In mice, CO_2 produces freezing and avoidance behavior that has been suggested to depend on the amygdala. However, a recent study in humans with bilateral amygdala lesions revealed that CO_2 can trigger fear and panic even in the absence of amygdalae, suggesting the importance of extra-amygdalar brain structures. Because the bed nucleus of the stria terminalis (BNST) contributes to fear- and anxiety-related behaviors and expresses acid-sensing ion channel-1A (ASIC1A), we hypothesized that the BNST plays an important role in CO_2-evoked fear-related behaviors in mice. We found that BNST lesions decreased both CO_2-evoked freezing and CO_2-conditioned place avoidance. In addition, we found that CO_2 inhalation caused BNST acidosis and that acidosis was sufficient to depolarize BNST neurons and induce freezing behavior; both responses depended on ASIC1A. Finally, disrupting *Asic1a* specifically in the BNST reduced CO_2-evoked freezing, whereas virus-vector-mediated expression of ASIC1A in the BNST of *Asic1a*$^{-/-}$ and *Asic1a*$^{+/+}$ mice increased CO_2-evoked freezing. Together, these findings identify the BNST as an extra-amygdalar fear circuit structure important in CO_2-evoked fear-related behavior.

Key words: **anxiety; ASIC1A; bed nucleus of the stria terminalis; CO2; panic; pH**

Introduction

Carbon dioxide (CO_2) inhalation causes anxiety, fear, and panic in humans, and these responses are heightened in patients with panic disorder (Esquivel et al., 2008). CO_2 concentrations from 5% to 35% have been used to demonstrate CO_2 sensitivity in panic disorder (Rassovsky and Kushner, 2003). Thus, CO_2 provides a valuable experimental tool with which to provoke and study panic. A better understanding of the neuroanatomical and molecular basis of CO_2 responses may provide critical insight into the mechanisms underlying panic.

The neuroanatomy underlying CO_2-defensive responses remains unclear. The amygdala, in keeping with its role in other defensive responses (Phelps and LeDoux, 2005), has been hypothesized to play a critical role in panic and CO_2-evoked responses (Gorman et al., 2000). Functional neuroimaging supports amygdala involvement, as both hypercapnia and dyspnea have been suggested to activate the amygdala (Brannan et al., 2001; Liotti et al., 2001; Evans et al., 2002). Further support for the amygdala in CO_2 responses was also provided by recent mouse studies, in which amygdala manipulations altered CO_2-evoked behavior (Ziemann et al., 2009). However, a 35% CO_2 inhalation challenge surprisingly elicited panic attacks and feelings of fear, anxiety, and panic in human patients with bilateral amygdala lesions (Feinstein et al., 2013). Together, these observations suggest that the amygdala is key in regulating CO_2-evoked defensive responses, but also underscore the possibility that structures outside of the amygdala may be critical.

The bed nucleus of the stria terminalis (BNST) is one extra-amygdalar structure that might contribute to CO_2-evoked fear and anxiety. Supporting a possible role for the BNST in CO_2-evoked behavior is the observation that the BNST exhibits relatively dense expression of acid-sensing ion channels (ASICs) (Coryell et al., 2007; Price et al., 2014), which have been implicated in CO_2 responses (Ziemann et al., 2009). Deleting *Asic1a* or *Asic2* in mice significantly attenuated CO_2-evoked freezing and CO_2 aversion (Ziemann et al., 2009; Price et al., 2014). These observations were consistent with previous studies, which found that *Asic1a*$^{-/-}$ and *Asic2*$^{-/-}$ mice have deficits in fear- and anxiety-related behaviors, such as cued and context fear conditioning and predator odor-evoked freezing (Wemmie et al., 2003; Coryell et al., 2007; Price et al., 2014; but see Pidoplichko et al.,

Received April 25, 2014; revised May 31, 2014; accepted June 13, 2014.

Author contributions: R.J.T., C.J.K., and J.A.W. designed research; R.J.T., Y.L., Y.W., C.J.K., A.G., R.F., and L.P.S. performed research; R.J.T. and Y.L. analyzed data; R.J.T. and J.A.W. wrote the paper.

J.A.W. was supported by the Department of Veterans Affairs (Merit Award), the National Institute of Mental Health (5R01MH085724), National Heart, Lung, and Blood Institute (R01HL113863), and a National Alliance for Research on Schizophrenia and Depression Independent Investigator Award. C.J.K. was supported by National Institute of Neurological Disorders and Stroke Training Grant T32NS045549. We thank John Freeman, George Richerson, Michael Welsh, Jason Allen, and Amanda Wunsch for their recommendations and assistance; and the University of Iowa Central Microscopy Facility and Gene Transfer Vector Core.

The authors declare no competing financial interests.

Correspondence should be addressed to Dr. John A. Wemmie, Roy J. and Lucille A. Carver College of Medicine, University of Iowa, Iowa City, IA 52242. E-mail: john-wemmie@uiowa.edu.

DOI:10.1523/JNEUROSCI.1680-14.2014

 0270-6474/14/3410247-09$15.00/0

2014). ASICs are trimeric, proton-gated cation channels of the DEG/ENaC family that are activated by extracellular acidosis (Waldmann et al., 1997; Wemmie et al., 2013). ASIC1A and ASIC2A are localized to dendritic spines and have previously been implicated in synaptic plasticity (Zha et al., 2006, 2009). Relatively little is known about the function of ASICs in humans, although polymorphisms in *Asic1a* and Asic2 have been recently associated with panic disorder, amygdala volume, and function (Gregersen et al., 2012; Smoller et al., 2014).

Because of the importance of the BNST in fear and anxiety, we hypothesized that the BNST contributes to CO_2-evoked behavior. Furthermore, because ASIC1A is critical for CO_2-evoked responses in mice, and ASIC1A is enriched in the BNST, we hypothesized that ASIC1A in the BNST may play a key role in these responses.

Materials and Methods

Mice. *Asic1a*$^{-/-}$ mice were generated as previously described (Wemmie et al., 2002) and maintained on a C57BL/6J congenic background. *Asic1a*$^{loxP/+}$ mice were generated by Xenogen Biosciences and intercrossed to produce *Asic1a*$^{loxP/loxP}$ mice. In brief, a targeting vector was designed in which exon 2 of *Asic1a* was flanked by loxP sites. A neomycin resistance cassette was also inserted to facilitate positive selection of electroporated embryonic stem cells and was later removed by flippase trasfection. *Asic1a*$^{loxP/loxP}$ mice were generated and maintained on a C57BL/6T congenic background. Because wild-type C57BL/6T mice froze more to 10% CO_2 than their C57BL/6J counterparts, it was important that experimental groups were matched with controls of the same congenic background. All mice were kept on a 12 h light-dark cycle, with all experiments being performed during the light cycle. Mice were fed standard chow and water *ad libitum*. Both male and female mice were used, and all experimental groups were sex- and age-matched. Mice undergoing behavioral testing were 12–18 weeks in age. Animal care met the standards set by the National Institutes of Health, and all experiments were approved by the University of Iowa Animal Care and Use Committee.

Electrolytic lesions. Mice were anesthetized with a mixture of ketamine and xylazine. A burr hole was drilled, and an electrode (an insect pin coated with epoxylite) was stereotaxically inserted into the BNST. The coordinates used to target the BNST were as follows: 0.4 mm anterior to bregma, 1.0 mm lateral to the midline, and 4.3 mm ventral from the pial surface. Bilateral lesions were made by passing 1.0 mA of DC through the electrode for 10 s per side. Mice were sutured and allowed to recover for at least 5 d before undergoing behavioral testing. Sham surgeries were performed as described above, but without insertion of the electrode into the BNST. Targeting was confirmed postmortem with Nissl staining and mapped (see Fig. 1*A*).

CO_2-evoked freezing. CO_2-evoked freezing was assessed as previously described (Ziemann et al., 2009; Price et al., 2014). Briefly, mice were placed in a Plexiglas chamber containing 10% CO_2 (10% CO_2, 21% O_2, balanced with N_2) for 10 min. Gas was infused at a flow rate of 5 L/min. Behavior was videotaped and scored by an observer blinded to genotype and condition. Freezing was defined as the absence of motion other than respiration.

CO_2-conditioned place avoidance. Custom avoidance chambers were constructed, each chamber with two sides (7.25 inches long × 5.5 wide × 7.5 tall), divided by a removable separator, and each side with distinct contextual cues: one side with black walls and a rod floor, and the other with white walls and a mesh floor. For gas flow, each side had an (0.25 inch) inlet and an (0.125 inch) outlet port. Gas was infused at a flow rate of 10 L/min. A 5 d protocol was used. On the first day, mice were allowed to freely explore both sides of the chamber for 20 min, and their behavior was videotaped. Time spent on each side was quantified by an observer blinded to genotype and condition; mice spending >70% of the time on either side at baseline were excluded. On days 2–4, mice underwent two training periods per day: one in the morning and one in the afternoon. During this time, mice were confined to one side of the chamber while being exposed to either 10% CO_2 (10% CO_2, 21% O_2, balanced with N_2) or compressed air. The context paired with CO_2 and order of CO_2 exposure were counterbalanced. On day 5, the mice were again allowed to freely explore both sides of the chamber, and the amount of time spent on the side previously paired with CO_2 was quantified. Conditioned place avoidance was determined by subtracting the time spent on the CO_2-paired side on day 1 from the time spent on the CO_2-paired side on day 5.

Locomotor testing. Total locomotion was assessed in the open field in room air as previously described (Coryell et al., 2007). In brief, mice were placed in an open field chamber measuring 40.6 × 40.6 × 36.8 cm (San Diego Instruments). Beam breaks were quantified over 30 min. Center activity was defined as the percentage of total beam breaks occurring in the center of the open field (25.5 × 25.5 cm) relative to total beam breaks.

Plethysmography. Ventilation was measured using standard plethysmographic techniques as previously described (Hodges et al., 2008) in a Buxco chamber with continuous gas flow (700 ml/min). The protocol consisted of >10 min of baseline in 0% CO_2/50% O_2, balanced with N_2, followed by exposures to 5%, 7%, and 10% CO_2, all containing 50% O_2, and balanced with N_2. All data were acquired using custom-written MATLAB (MathWorks) software. All data segments ≥5 s in duration that did not contain sighs, sniffing, or movement artifacts were selected for analysis. At least 40 s of data was analyzed for each gas. All analyzed data were obtained after 60 s of gas exposure to ensure equilibrium in the chamber. Relative minute ventilation is reported, normalized to sham mice in 0% CO_2/50% O_2.

Immunohistochemistry and imaging. Fresh tissue was embedded in OCT (Tissue-Tek) and frozen. The 18 μm coronal sections were sliced and mounted onto slides using the CryoJane system (Leica Biosystems). eGFP was imaged directly without use of antibodies. For ASIC1A immunohistochemistry, sections were postfixed in PBS with 4% PFA and 4% sucrose for 10 min, followed by three 5 min washes with PBS. Sections were then permeabilized with a 5 min exposure to 0.25% Triton X-100 in PBS, followed by three 5 min washes with PBS. Sections were blocked for 1 h in 5% goat serum and then incubated overnight at 4°C with rabbit polyclonal anti-ASIC1 antiserum (MTY19) (Wemmie et al., 2003) diluted 1:1000 in 5% goat serum Sections were washed three times for 5 min in PBS, followed by a 1 h incubation with goat-anti rabbit IgG antibody coupled to AlexaFluor-488 or AlexaFluor-568 (Invitrogen) diluted 1:500 in goat serum. Sections were washed three times for 5 min in PBS and mounted with Vectashield (Vector Labs). Sections were imaged at 10× using a Zeiss confocal microscope (Zeiss 710). Colabeling with ASIC1A and mouse monoclonal NeuN antibody (Millipore) and mouse monoclonal GFAP antibodies (Millipore) was done in a similar manner. NeuN was diluted 1:250, and GFAP was diluted 1:500 and then detected with a goat-antimouse antibody coupled to AlexaFluor-568 (Invitrogen). Sections were imaged at 20×.

Preparation of acute BNST slices. Coronal BNST brain slices (300 mM) were prepared from 8- to 12-week-old mice, in accordance with the University of Iowa guidelines. Briefly, BNST slices were cut using a Vibratome 1000 Plus (Vibratome) in ice-cold slicing buffer (in mM as follows: 127 NaCl, 26 $NaHCO_3$, 1.2 KH_2PO_4, 1.9 KCl, 1.1 $CaCl_2$, 2 $MgSO_4$, 10 D-glucose) bubbled with 95% O_2 and 5% CO_2. Slices were then transferred to a holding chamber containing oxygenated ACSF (in mM as follows: 127 NaCl, 26 $NaHCO_3$, 1.2 KH_2PO_4, 1.9 KCl, 2.2 $CaCl_2$, 1 $MgSO_4$, 10 D-glucose) for 30 min at 34°C and for another 30 min at 22°C for recovery, and then transferred to a submersion recording chamber continually perfused with 32°C oxygenated ACSF (rate: 2 ml/min). Slices were equilibrated for at least 15 min before each recording.

Electrophysiology. Whole-cell recordings from BNST neurons were made using an Axopatch 200B amplifier (Molecular Devices), sampled at 10 kHz, digitized by a DigiData 1322A, and later analyzed off-line by ClampFit (Axon software). Recording pipettes with resistances ranging between 3 and 6 Mohms were pulled using standard borosilicate capillaries by a Flaming-Brown electrode puller (P-97, Sutter Instruments) and were filled with a K-gluconate-based patch solution (in mM as follows: 125 K-gluconate, 20 KCl, 10 NaCl, 2 Mg-ATP, 0.3 Na-GTP, 2.5 QX314, 10 HEPES, 0.2 EGTA, pH 7.3 adjusted with KOH) for the measurement of acid-evoked currents. A different pipette solution (in mM as follows: 130 K-gluconate, 1 $MgCl_2$, 5 Mg-ATP, 0.4 Na-GTP, 10 HEPES, 5

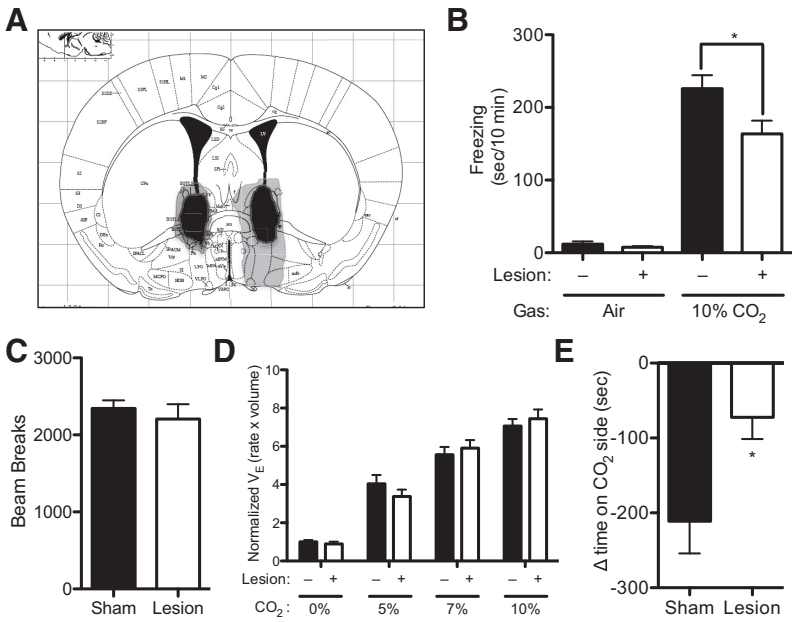

Figure 1. BNST lesions reduce CO_2-evoked behavior. ***A***, Diagram representing location and size of the largest (gray) and smallest (black) lesions (Paxinos and Franklin, 2001). ***B***, BNST lesions reduced CO_2-evoked freezing. ***C***, BNST lesions significantly reduced conditioned avoidance to CO_2. ***D***, BNST lesions did not alter minute ventilation (V_E). ***E***, BNST lesions did not alter locomotion in the open field.

EGTA, pH 7.3 adjusted with KOH) was used for current-clamp experiments. A total of 20 mM CNQX was used to block AMPA receptors, 100 mM picrotoxin was used to block $GABA_A$ receptors, and 100 mM APV was used to block NMDA receptors.

Western blotting. Tissue punches for Western blotting were taken bilaterally from the BNST, and homogenized. 7.5 μg lysate was run on a Bis-Tris gel and transferred to a PVDF membrane for Western blotting. Primary antibodies used were as follows: rabbit polyclonal anti-ASIC1 antiserum (MTY19) (Wemmie et al., 2003) diluted 1:500 and chicken polyclonal anti-GAPDH antibody (Millipore) diluted 1:10,000. Secondary antibodies used were as follows: IRDye 800CW donkey anti-rabbit IgG (LI-COR) and IRDye 680LT Donkey anti-chicken IgG (LI-COR), both diluted 1:10,000. The blots were imaged with the Odyssey imaging system (LI-COR).

Fiberoptic pH sensors. Mice were anesthetized with a mixture of ketamine and xylazine. A burr whole was drilled and a fiberoptic pH sensor (World Precision Instruments) was implanted into the BNST. The following coordinates were used to target the BNST: 0.4 mm anterior from bregma, 1.0 mm lateral from the midline, and 4.3 mm ventral from the pial surface. After pH readings stabilized for at least 10 min, mice were then exposed to increasing doses of CO_2 (5%, 10%, 20%) for 10 min, with a 10 min recovery period between doses. Simultaneous measurement of and delivery of acid into the BNST was accomplished by either affixing an injector <1 mm from the tip of the pH sensor and implanting it into the BNST, or cannulating the BNST for acid infusion and implanting a pH sensor into the amygdala. The following coordinates were used to target the amygdala: 1.5 mm posterior to bregma, 3.5 mm lateral to the midline, and 4.5 mm the from skull surface at bregma.

BNST cannulae. Cannulae were sterotaxically implanted into the BNST in a manner similar to that which has been previously described (Coryell et al., 2009; Ziemann et al., 2009). Briefly, a 25 gauge guide cannula was implanted into the BNST. The following coordinates were used to target the BNST: 0.4 mm anterior to bregma, 1.0 mm lateral to the midline, and 3.5 mm ventral from pial surface. Mice recovered from surgery for at least 3 d. A 30 gauge injector was inserted into guide cannula, extending 1 mm past the cannula tip; 1 μl of ACSF (either pH 3.0 or pH 7.3) was infused over 5–10 s. Because of the rapid buffering capacity of the brain, it was necessary to inject such an acidic solution (pH 3) to lower the pH of the tissue to ~6.8. Mice were immediately placed in a Plexiglas behavior chamber and the behavioral response was videotaped for 10 min. A blinded observer scored freezing, which was defined as an absence of movement except for respiration. Cannula targeting was confirmed postmortem with a dye infusion.

Viral injections. Adeno-associated virus (AAV) vectors were obtained from the University of Iowa Gene Transfer Vector Core and injected as previously described (Coryell et al., 2008, 2009; Ziemann et al., 2009). All viruses used were AAV2/1 chimeric viruses, with a CMV promoter driving expression of ASIC1A, Cre recombinase, or eGFP. AAV-*cre* and AAV-*Asic1a* were coinjected with AAV-*eGFP* to aid with localization. A total of 0.5 μl of virus was injected into each site. The BNST coordinates were (relative to bregma): anteroposterior 0.4 mm, lateral $\pm$1.0 mm, ventral 4.3 mm from the pial surface. Hippocampus coordinates were (relative to bregma): anteroposterior $-$1.5 mm, lateral 1 mm, and ventral 1.5 mm from pial surface. Mice were allowed to recover for at least 3 weeks before behavioral testing. Targeting was determined postmortem. Bilateral transduction in the BNST was required to be categorized as a hit and misses and unilateral hits were excluded from further analysis.

Statistical analysis. All values are plotted as mean $\pm$ SEM. Significance between two groups with equal variance was tested using a Student's *t* test. Significance between two groups with unequal variance was tested using a Student's *t* test with Welch's correction. Significance between more than two groups was tested using an ANOVA. Within the context of the ANOVA, planned contrast testing (Student's *t* test) and *post hoc* testing (Bonferroni's multiple-comparison test) were performed to test for differences between two groups. For all tests, $p < 0.05$ was considered significant. Analyses were performed using Prism software (GraphPad).

Results

CO_2-evoked behaviors depend on the BNST

Although the role of the BNST in humans is not fully understood, recent human functional imaging studies are consistent with BNST involvement in anxiety (Somerville et al., 2010, 2013; Alvarez et al., 2011; Grupe et al., 2013; Avery et al., 2014). Rodent studies have also implicated the BNST in fear-and anxiety-related behaviors, particularly unconditioned fear responses, such as to predator odors (LeDoux et al., 1988; Lee and Davis, 1997; Fendt et al., 2003; Sullivan et al., 2004). Much as predator odors herald the potential threat of predation, CO_2 heralds the potential threat of suffocation; thus, CO_2 might act as an unconditioned aversive stimulus that engages the BNST. Previous studies used bilateral electrolytic lesions to implicate the BNST in rodent models of fear and anxiety (Sullivan et al., 2004; Luyten et al., 2011). Therefore, to test the hypothesis that the BNST might contribute to CO_2-evoked behaviors, we bilaterally lesioned the BNST. These lesions hit both the dorsal and ventral aspects of the BNST, including the oval and anterodorsal subnuclei (Fig. 1*A*). Because freezing is a widely used measure of fear-related behavior, and because previous studies suggested that 10% CO_2 evokes a robust freezing response in wild-type C57BL/6J mice (Ziemann et al., 2009), we tested 10% CO_2-evoked freezing in BNST-lesioned mice versus sham controls. We found that 10% CO_2 induced prominent freezing behavior that was absent in compressed air (Fig. 1*B*)

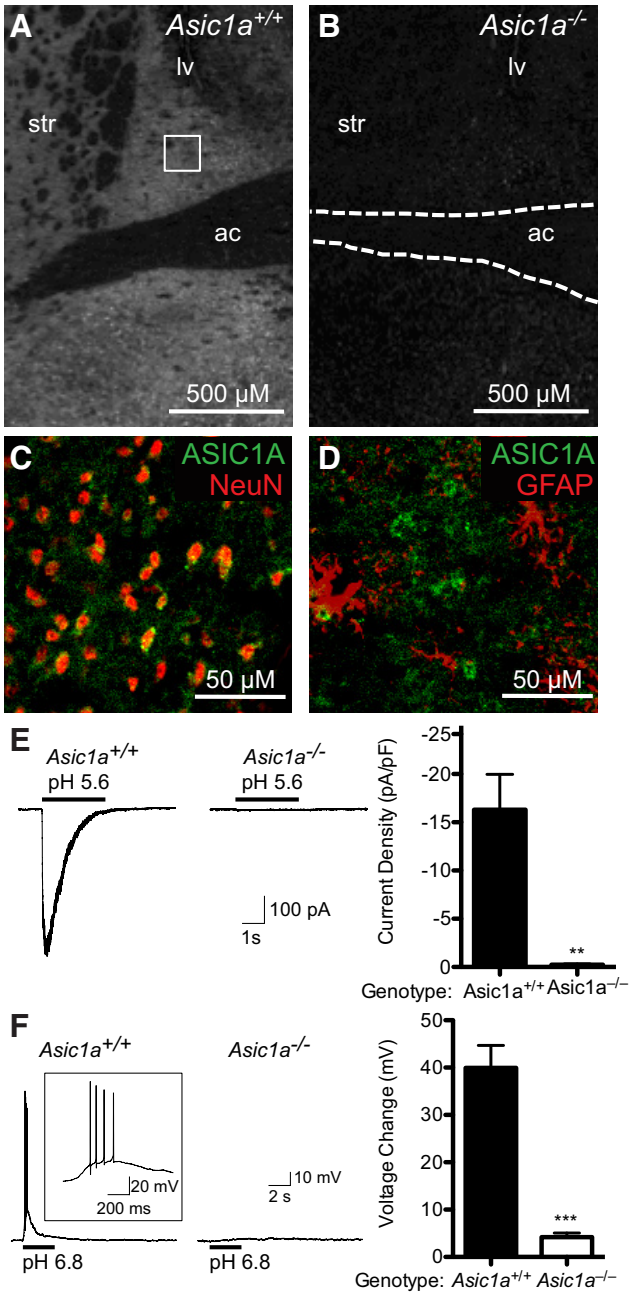

Figure 2. ASIC1A is expressed in the BNST and is critical for acid-evoked currents and depolarization. ***A***, ***B***, ASIC1A immunofluorescent labeling (white) in the BNST of *Asic1a* $^{+/+}$ versus *Asic1a* $^{-/-}$ mice. The lateral ventricle (lv), striatum (str), and anterior commissure (ac) are labeled for reference. Square represents region analyzed in different slices for NeuN and GFAP immunohistochemistry (bottom). ***C***, Immunofluorescent labeling of ASIC1A (green) and NeuN (red) in the BNST of an *Asic1a* $^{+/+}$ mouse. ***D***, Immunofluorescent labeling of ASIC1A (green) and GFAP (red) in the BNST of an *Asic1a* $^{+/+}$ mouse. ***E***, Whole-cell voltage-clamp recording of BNST neurons in slices. pH 5.6 evoked currents in BNST neurons in slices from *Asic1a* $^{+/+}$ but not *Asic1a* $^{-/-}$ mice. ***F***, Whole-cell current-clamp recording of BNST neurons in slices. pH 6.8 elicited depolarization and action potentials in *Asic1a* $^{+/+}$ neurons but not *Asic1a* $^{-/-}$ neurons.

($F_{(1,37)} = 152.1$, $p < 0.0001$). Moreover, BNST lesions significantly attenuated CO_2-evoked freezing, although they did not completely abolish it (Fig. 1*B*) ($p = 0.0271$).

To further probe the role of the BNST in CO_2-evoked behavior, we developed a CO_2 conditioned place avoidance assay (CO_2-CPA), in which mice learn to associate 10% CO_2 with a specific context in a two-sided box and subsequently avoid it when given a choice between the context previously paired with CO_2 versus one previously paired with compressed air (see Materials and Methods). Because the BNST has been suggested to play a role in contextually conditioned fear (Sullivan et al., 2004), we hypothesized that BNST lesions would impair CO_2-CPA. We found that both BNST- and sham-lesioned animals avoided the context previously paired with CO_2. Consistent with our hypothesis, BNST lesions significantly reduced CO_2-conditioned place avoidance (Fig. 1*C*) ($t_{(11)} = 2.580$, $p = 0.0256$, $n = 7$, $n = 6$).

In light of a recent study implicating the BNST in control of respiratory rate (Kim et al., 2013) and because elevated CO_2 concentrations (hypercapnia) potently stimulate breathing (Hodges et al., 2008), we further sought to determine whether BNST lesions might alter the hypercapnic ventilatory response. Inhaling 5%, 7%, and 10% CO_2 increased minute ventilation (V_E) to increasing degree (Fig. 1*D*) ($F_{(3,68)} = 422.8$, $p < 0.0001$ $n = 10$, $n = 9$). However, BNST lesions did not interfere with this response ($F_{(1,68)} = 0.002381$, $p = 0.9657$), and there was no $CO_2 \times$ lesion interaction ($F_{(3,68)} = 3.435$, $p = 0.4471$). We also assessed locomotion by quantifying total beam breaks in open field test and found that the BNST-lesioned mice were similar to their sham counterparts (Fig. 1*E*) ($t_{(20)} = 0.6284$, $p = 0.5369$), and no difference was detected in center activity (sham 34.45 ± 1.451%, lesion 30.93 ± 1.680%, $t_{(20)} = 1.586$, $p = 0.1283$). These results suggest that effects of BNST lesions on unconditioned and conditioned behavioral responses to 10% CO_2 are not driven by differences in CO_2-induced hyperventilation or by general differences in locomotion.

ASIC1A in BNST neurons is critical for acid-evoked currents and depolarization

Because previous studies suggested that ASIC1A contributes to CO_2 detection in the amygdala and because ASIC1A was previously detected in the BNST (Coryell et al., 2007; Price et al., 2014), we hypothesized that ASIC1A in the BNST might contribute to CO_2-evoked behavior. We confirmed the presence of ASIC1A in BNST neurons using ASIC1A immunohistochemistry in *Asic1a* $^{+/+}$ versus *Asic1a* $^{-/-}$ mice (Fig. 2*A*,*B*) and by taking advantage of colocalization with the neuronal marker NeuN (Fig. 2*C*). We found that a substantial component of the ASIC1A signal overlapped with NeuN at neuron somata. We also observed an ASIC1A-specific extrasomatic signal that did not overlap with the astrocyte marker GFAP (Fig. 2*D*), which is most likely consistent with the previously established localization of ASIC1A in dendrites (Wemmie et al., 2002; Hruska-Hageman et al., 2004; Zha et al., 2006, 2009). Next, we tested for ASIC1A-dependent channel activity using a relatively severe acid challenge, pH 5.6. We found that this challenge evoked large currents from BNST neurons in *Asic1a* $^{+/+}$ slices. Whereas BNST neurons from *Asic1a* $^{-/-}$ mice lacked this acid-evoked current (Fig. 2*E*) ($t_{(6)} = 4.364$, $p = 0.0048$, $n = 7$, $n = 6$), membrane capacitance was not different across genotypes (*Asic1a* $^{+/+}$ 49.09 ± 3.114 pF, $n = 28$; *Asic1a* $^{-/-}$ 49.04 ± 2.460 pF, $n = 24$: $t_{(50)} = 0.01259$, $p = 0.9900$). Thus, even severe acidosis failed to evoke current in BNST neurons from *Asic1a* $^{-/-}$ mice. A more physiologic challenge, pH 6.8, induced depolarization and action potentials in *Asic1a* $^{+/+}$ neurons assessed by whole-cell current clamp, but not in *Asic1a* $^{-/-}$ neurons (Fig. 2*F*) ($t_{(5)} = 7.385$, $p = 0.0007$, $n = 6$, $n = 7$).

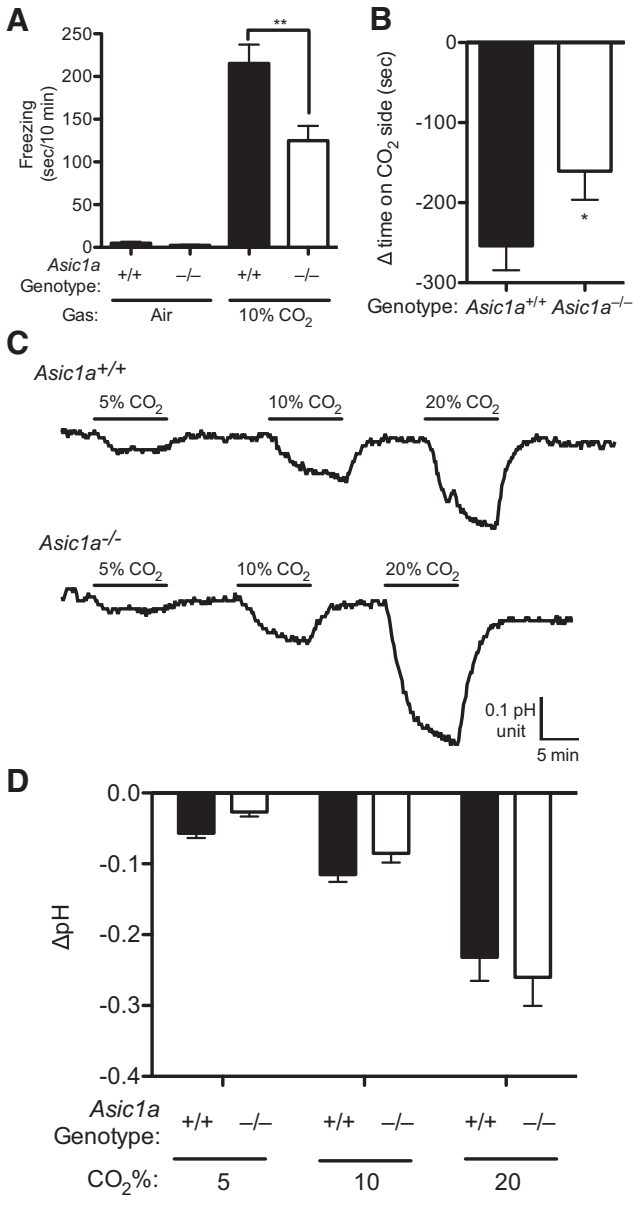

Figure 3. CO_2 inhalation causes freezing, avoidance, and BNST acidosis. ***A***, Freezing behavior in air versus 10% CO_2. CO_2 elicited freezing, which was attenuated in the *Asic1a*$^{-/-}$ mice. ***B***, CO_2-conditioned place avoidance, measured as a change in time spent on target side after conditioning relative to pretest, was significantly attenuated in *Asic1a*$^{-/-}$ mice relative to *Asic1a*$^{+/+}$ mice. ***C***, Representative traces of pH recordings measured by fiberoptic pH sensor implanted in the BNST. Inhaling the indicated concentrations of CO_2 induced acidosis in both *Asic1a*$^{+/+}$ and *Asic1a*$^{-/-}$ mice. ***D***, Mean pH responses to CO_2 were similar in *Asic1a*$^{+/+}$ and *Asic1a*$^{-/-}$ mice.

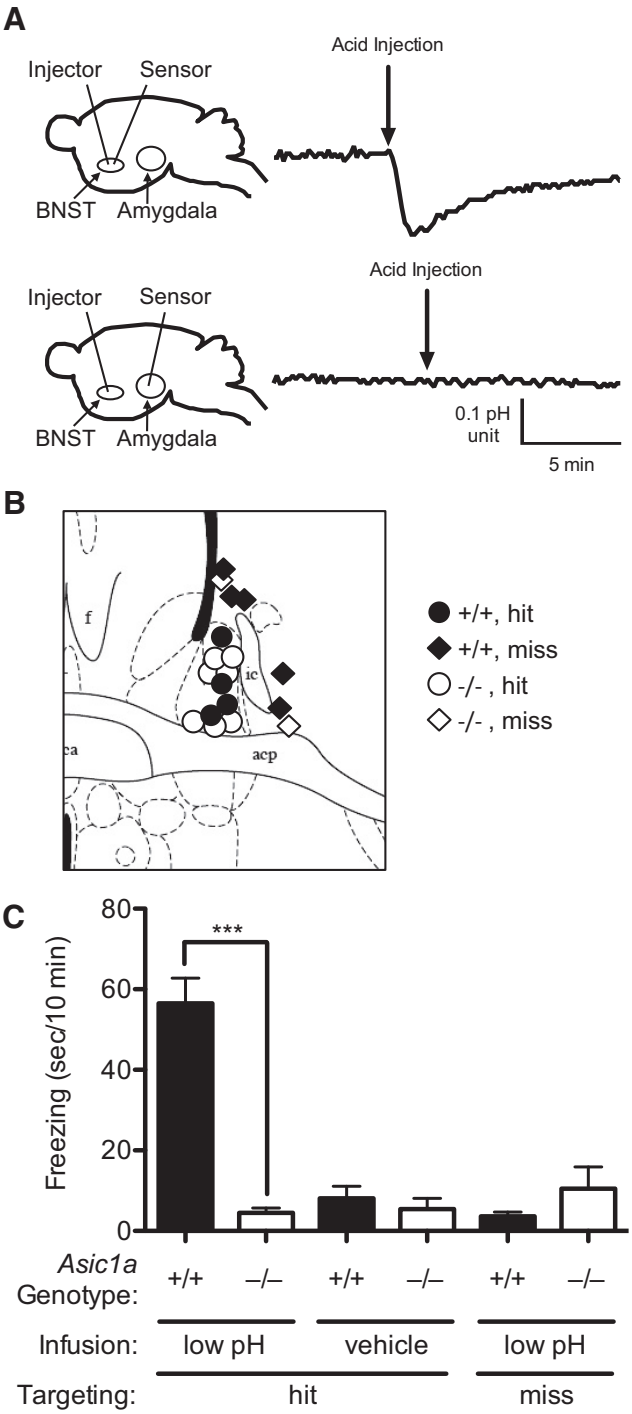

Figure 4. BNST acidosis evokes ASIC1A-dependent freezing. ***A***, Schematic of experimental design with fiberoptic pH sensors implanted in BNST or amygdala, showing that infusion of low pH solution into the BNST acidifies the BNST but not the amygdala. ***B***, Diagram of acid infusion sites; BNST (circles) versus extra BNST (diamonds) (Paxinos and Franklin, 2001). ***C***, Freezing behavior after infusion of low pH solution or normal pH solution in cases that hit or missed the BNST. Infusing low pH solution evoked a freezing response in ASIC1A$^{+/+}$ mice that was largely absent in *Asic1a*$^{-/-}$ mice. Low pH infusions into the BNST of *Asic1a*$^{+/+}$ mice evoked significantly more freezing than in *Asic1a*$^{-/-}$ mice. In *Asic1a*$^{+/+}$ mice, low pH infusions hitting the BNST elicited significantly more freezing than those that missed the BNST.

CO_2 causes freezing, conditioned avoidance, and BNST acidosis

Like BNST lesions, and consistent with previous observations (Ziemann et al., 2009; Price et al., 2014), we found that ASIC1A disruption attenuated both the freezing response to 10% CO_2 (Fig. 3*A*) ($F_{(1,39)} = 10.02$, $p = 0.0030$ gas × genotype interaction, $p = 0.0049$, $n = 11$, $n = 11$, $n = 11$, $n = 10$) and CO_2-CPA (Fig. 3*B*) ($t_{(36)} = 1.977$, $p = 0.0279$, $n = 19$, $n = 19$, one-tailed). To explore how CO_2-induced behavior might depend on the BNST and ASICs, we measured pH in the BNST of anesthetized mice with a fiberoptic pH sensor. When the mice were breathing only compressed air, average pH was 6.93 ± 0.12 and 6.85 ± 0.08 in *Asic1a*$^{+/+}$ and *Asic1a*$^{-/-}$ mice, respectively ($t_{(4)} = 0.5153$, $p = 0.63$, $n = 3$ per group). These values are consistent with previous pH measurements in the lateral ventricle and amygdala using the same approach, and are less than what might be expected in

awake animals (pH 7.29–7.39) (Mitchell et al., 1965; Mayhan et al., 1988) likely due to anesthesia-induced respiratory suppression and the associated hypercarbia (Ziemann et al., 2009). Increasing concentrations of inhaled CO_2 to 5%, 10%, and 20% lowered pH in the BNST to increasing degree (Fig. 3*C*,*D*) ($F_{(2,12)} = 42.47, p < 0.0001, n = 3, n = 3$). However, *Asic1a* disruption did not alter this response ($F_{(1,12)} = 0.3209, p = 0.5815$), and there was no gas × genotype interaction ($F_{(2,12)} = 1.089, p = 0.3677$). The magnitude of the acidosis in the two genotypes was not different, suggesting that ASIC1A disruption does not alter pH (Ziemann et al., 2009). Conceivably, respiratory suppression due to anesthesia may obscure the absolute pH changes evoked by CO_2 inhalation. Nevertheless, these measurements grossly confirm CO_2-induced acidosis in the BNST and provide a useful estimate of the pH changes.

BNST acidosis evokes freezing that depends on ASIC1A

To test whether acidosis in the BNST might be sufficient to trigger behavior, we directly infused acidic ACSF into the BNST of *Asic1a*$^{+/+}$ and *Asic1a*$^{-/-}$ mice. We found that infusing ACSF pH 3 into the BNST of anesthetized mice lowered pH by a magnitude approximately similar to that observed during 10% CO_2 inhalation (Fig. 4*A*). Importantly, delivering acidic ACSF to the BNST did not alter pH in the basolateral amygdala (Fig. 4*A*), a location where acidic pH has been previously shown to evoke freezing behavior (Ziemann et al., 2009). We next tested effects of infusions through guide cannulae into the BNST of awake, behaving mice (Fig. 4*B*) and found a significant genotype × infusion interaction (Fig. 4*C*) ($F_{(1,18)} = 60.81, p < 0.0001$). Like CO_2 inhalation, direct acidification of the BNST evoked freezing behavior in *Asic1a*$^{+/+}$ mice relative to vehicle pH 7.3 (Fig. 4*C*) ($t_{(8)} = 7.81, p < 0.001$). However, this response was absent in *Asic1a*$^{-/-}$ mice ($t_{(10)} = 0.347, p = 0.74$). Acidic infusions that missed the BNST also failed to evoke freezing behavior (Fig. 4*C*) ($t_{(6)} = 1.40, p = 0.210$). Together, these data suggest that the BNST is sensitive to pH and that the ability of CO_2 to evoke freezing behavior may come, at least in part, through direct acidification of the BNST.

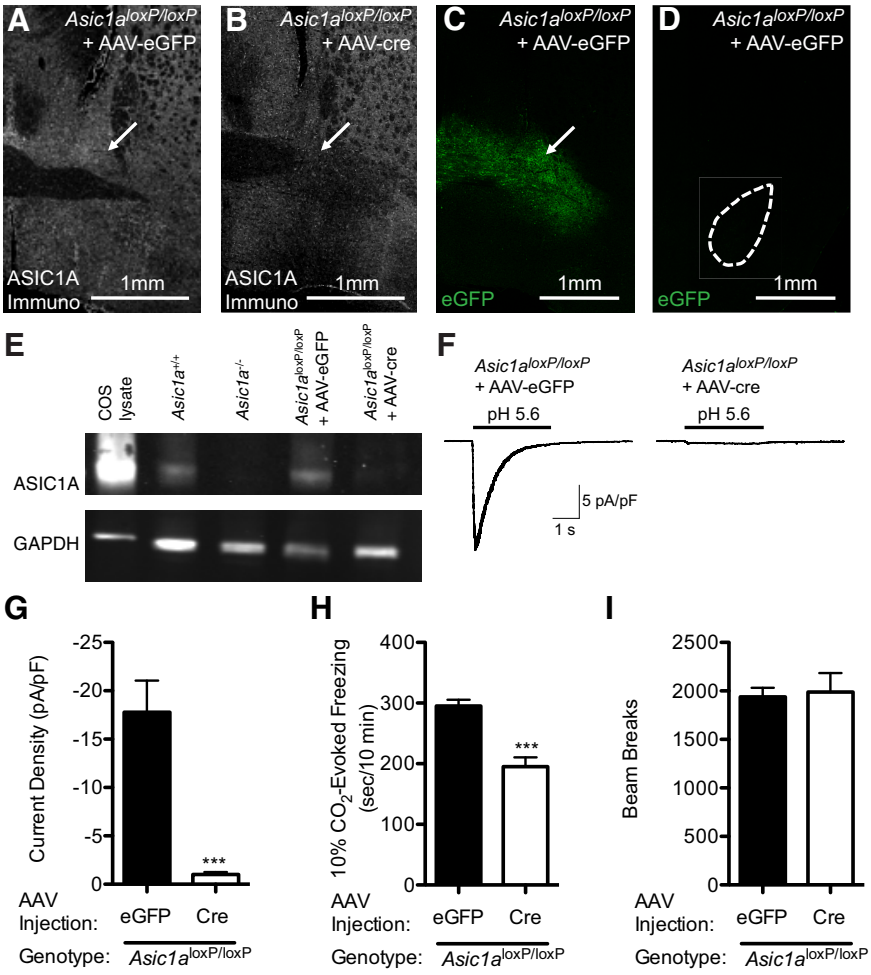

Figure 5. Disrupting ASIC1A in the BNST reduces acid-evoked currents and CO_2-evoked freezing. ***A***, ***B***, Examples of ASIC1A immunofluorescent labeling (white) of *Asic1a*$^{loxP/loxP}$ mice injected with AAV-eGFP or AAV-cre into the BNST (arrow), showing a localized disruption of ASIC1A expression in the AAV-cre injected BNST. ***C***, ***D***, In the same mouse, AAV-eGFP transduction in the BNST produced eGFP expression (green) in the BNST (arrow), but not in the basolateral amygdala (dashed circle). ***E***, Western blot of ASIC1A protein from Cos cells transfected with *Asic1a* and from BNST punches from mice of the indicated genotypes and virus transduction. AAV-cre injections eliminated the majority of the ASIC1A protein in the BNST. GAPDH immunoblotting was included as a loading control. ***F***, ***G***, Whole-cell voltage-clamp recordings of neurons from BNST slices. AAV-cre disrupted acid-evoked currents in the BNST of *Asic1a*$^{loxP/loxP}$ mice. ***H***, Quantification of freezing behavior evoked by 10% CO_2. AAV-cre injections into the BNST of *Asic1a*$^{loxP/loxP}$ mice significantly reduced freezing. ***I***, AAV-cre transduction in the BNST of *Asic1a*$^{loxP/loxP}$ mice did not alter locomotion in the open field relative to AAV-eGFP transduced controls.

ASIC1A in the BNST is required for normal CO_2-evoked freezing

To test whether the BNST is a key site of ASIC1A action in CO_2-evoked behavior, we took advantage of a mouse with loxP sites inserted into the introns flanking the critical second exon of the *Asic1a* gene (*Asic1a*$^{loxP/loxP}$). Expressing Cre recombinase in the BNST of these mice via an adeno-associated virus vector (AAV-Cre) removed exon 2 and disrupted ASIC1A as assessed by immunohistochemistry (Fig. 5*A*,*B*), Western blot (Fig. 5*E*), and acid-evoked currents (Fig. 5*F*,*G*) ($t_{(8)} = 5.086, p = 0.0009, n = 9, n = 8$). Whereas ASIC1A expression levels were intact in *Asic1a*$^{loxP/loxP}$ mice transduced with the AAV-eGFP control vector (Fig. 5*E*). Within the BNST, the viruses tended to transduce both the oval and anterodorsal nuclei (Fig. 5*B*,*C*). In contrast to our lesion studies, where we cannot rule out effects of fibers of passage, in this approach no virus transduction was detected in the basolateral amygdala (Fig. 5*D*), suggesting that the virus was not taken up by fibers from cells connected to the BNST (Kim et al., 2013) or by fibers passing through the BNST or anterior commissure (Martínez-Lorenzana et al., 2004). We next tested the effects of these viral manipulations on freezing behavior evoked by 10% CO_2. We found that CO_2-evoked freezing was significantly attenuated in *Asic1a*$^{loxP/loxP}$ mice in which the BNST was transduced with AAV-Cre relative to those transduced with AAV-eGFP (Fig. 5*H*) ($t_{(18)} = 5.532, p < 0.0001, n = 12, n = 8$). In contrast, general locomotor activity in the open field was un-

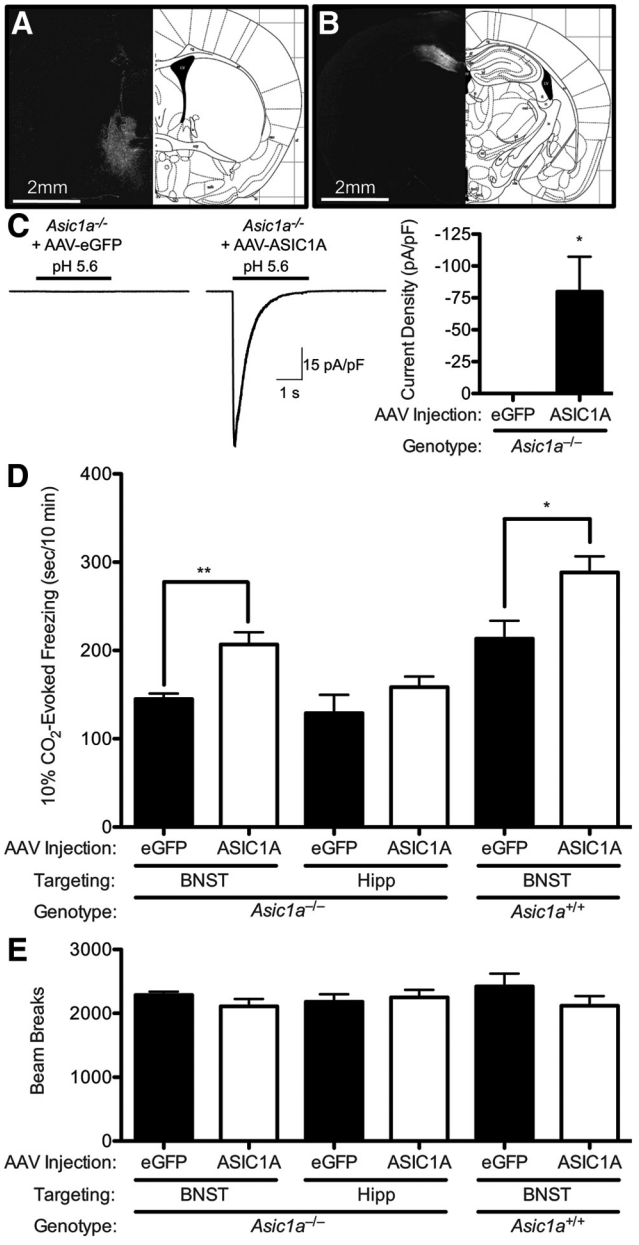

Figure 6. Expressing ASIC1A in the BNST is sufficient to increase CO_2-evoked freezing. ***A***, ASIC1A immunofluorescence in the BNST (white) of *Asic1a*$^{-/-}$ mice injected with AAV-ASIC1A. ***B***, ASIC1A immunofluorescence in the dorsal hippocampus (white) of *Asic1a*$^{-/-}$ mice injected with AAV-ASIC1A. ***C***, Whole-cell voltage-clamp recordings of neurons from BNST slices. AAV-ASIC1A produced acid-evoked currents in the BNST of *Asic1a*$^{-/-}$ mice. ***D***, Quantification of freezing evoked by 10% CO_2 in mice of indicated genotypes, viruses, and injection sites. In *Asic1a*$^{-/-}$ mice, AAV-ASIC1A in the BNST significantly increased freezing relative to AAV-eGFP injected controls, whereas AAV-ASIC1A in dorsal hippocampus (Hipp) did not. In *Asic1a*$^{+/+}$ mice, AAV-ASIC1A in the BNST significantly increased CO_2-evoked freezing relative to AAV-eGFP controls. ***E***, Infusion of AAV-ASIC did not alter locomotion in the open field.

affected by these manipulations (Fig. 5*I*) ($t_{(18)} = 0.2491$, $p = 0.8061$), and center activity was not significantly different (AAV-GFP 36.23 ± 2.354%, AAV-Cre 29.81 ± 1.498%, $t_{(18)} = 2.037$, $p = 0.0567$). These results suggest that CO_2-evoked freezing depends on ASIC1A in the BNST.

ASIC1A in the BNST is sufficient to increase CO_2-evoked freezing

The previous data suggested that ASIC1A in the BNST is necessary for normal CO_2-evoked freezing. To test whether ASIC1A in the BNST is also sufficient to increase CO_2-evoked freezing, we used an AAV vector expressing ASIC1A (AAV-ASIC1A) to drive ASIC1A expression to the BNST of *Asic1a*$^{-/-}$ mice. We found that the AAV-ASIC1A vector produced prominent ASIC1A protein expression (Fig. 6*A*) and acid-evoked currents in transduced neurons (Fig. 6*C*) ($t_{(6)} = 2.894$, $p = 0.0275$, $n = 9$, $n = 7$). Moreover, AAV-ASIC1A-injected *Asic1a*$^{-/-}$ mice had a significant increase in 10% CO_2-evoked freezing relative to their AAV-eGFP-injected counterparts (Fig. 6*D*) ($F_{(5,40)} = 13.10$, $p < 0.0001$, $n = 5$, $n = 9$, $n = 7$, $n = 7$, $n = 7$, $n = 8$, one-way ANOVA, $t_{(12)} = 3.165$, $p = 0.0081$). To test for site specificity, we also transduced the dorsal hippocampus with AAV-ASIC1A or AAV-eGFP (Fig. 6*B*) and found no effect on 10% CO_2-evoked freezing (Fig. 6*D*) ($t_{(12)} = 1.231$, $p = 0.2420$). Finally, to test whether we could use this system to exaggerate CO_2-evoked behavior, we injected AAV-ASIC1A versus AAV-eGFP into the BNST of *Asic1a*$^{+/+}$ mice. We found that, in the background of normal ASIC1A expression, targeting AAV-ASIC1A to the BNST was sufficient to significantly increase CO_2-induced freezing (Fig. 6*D*) ($t_{(13)} = 2.755$, $p = 0.0164$), whereas these manipulations did not significantly affect general locomotor activity (Fig. 6*E*) ($F_{(5,40)} = 0.7138$, $p = 0.1547$) or center activity ($F_{(5,40)} = 0.1.594$, $p = 0.1662$) in the open field.

Discussion

Our results identify the BNST as a key structure in CO_2-evoked fear-related behaviors. Not only does the BNST mediate CO_2-evoked freezing and conditioned avoidance, our data suggest that CO_2 acidifies the BNST and that the BNST can directly detect acidosis, through ASIC1A. These findings are consistent with a previously established role for the BNST in rodent models of unconditioned and conditioned fear (LeDoux et al., 1988; Lee and Davis, 1997; Fendt et al., 2003; Sullivan et al., 2004) and for ASICs in CO_2-evoked behavior (Ziemann et al., 2009; Price et al., 2014).

Several lines of evidence suggest that the BNST is pH sensitive. CO_2 inhalation lowers pH in the BNST. Explicitly and directly manipulating pH in the BNST evokes freezing behavior. A pH-sensitive channel, ASIC1A, is expressed in the BNST. And CO_2- and acidosis-evoked behaviors depend on ASIC1A. Together, these observations suggest that ASIC1A in the BNST directly detects CO_2-induced acidosis. However, we cannot rule out the possibility that acidosis activates some other pH-sensitive receptive mechanisms, which depend on ASIC1A in the BNST.

The observation that structures in the fear circuit are pH sensitive raises questions about the adaptive value of sensing pH deep within the CNS. By detecting rising CO_2 levels, the BNST and amygdala might alert the animal to a threat of suffocation (Klein, 1993). But why is CO_2 detection in the forebrain of value given that CO_2 and its diverse physiological effects can be detected or inferred through a variety of other mechanisms, such as smell (Hu et al., 2007), taste (Chandrashekar et al., 2009), and interoception (e.g., chest wall movement) (Flume et al., 1996), or inspiratory resistance (Lang et al., 2011)? Perhaps CO_2 sensitivity in the brain functions as a failsafe mechanism or as a last resort when other means of detecting suffocation and rising CO_2 are inadequate. Or perhaps the pH sensitivity in the fear circuit helps the organism recognize the experience of CO_2 inhalation as a danger. Or maybe pH sensitivity in deep CNS structures is a conserved vestige from simpler organisms (Cummins et al., 2014). Alternatively, pH-sensitive molecules may normally play other roles and might be serendipitously activated by CO_2. For example, ASICs are localized on dendritic spines (Zha et al.,

2006) and have been suggested to be activated by protons released during synaptic transmission (Wemmie et al., 2013). Regardless of these questions, the finding that multiple forebrain structures detect acidosis raises the possibility that brain pH may play a more general role in brain function and behavior.

One limitation of our lesion and viral studies is that they are not sufficiently precise to discern which BNST subnuclei are critical for CO_2-evoked freezing and conditioned avoidance. This could be particularly important as recent studies have suggested opposing roles for BNST subnuclei in anxiety-related behavior (Haufler et al., 2013; Kim et al., 2013). For example, Kim et al. (2013) found that the oval nucleus of the BNST (ovBNST) promoted anxiety-like behavior, whereas the anterodorsal BNST (adBNST) reduced anxiety-like behavior in the elevated plus maze. Nevertheless, our findings are consistent with other en masse manipulations of the BNST (LeDoux et al., 1988; Lee and Davis, 1997; Fendt et al., 2003; Sullivan et al., 2004; Kim et al., 2013). Although our current methods did not hit the ovBNST without hitting surrounding structures, infusing smaller volumes of virus might limit spread and increase site specificity. However, the apparent anxiety-promoting effects on CO_2-evoked behaviors detected here suggest that the ovBNST might be responsible.

The amygdala has also been implicated in CO_2-evoked behaviors (Ziemann et al., 2009; Feinstein et al., 2013). This, coupled with our results herein, raises questions about the respective roles of the BNST and amygdala and their potential relationship. Are these roles duplicative, or do these two structures play unique roles that we have not yet been able to discern? Do these structures function independently, or do they function together, perhaps in series? Established interconnections between the BNST and amygdala suggest that the two structures may function together as a part of a network (Davis, 2002; Walker and Davis, 2008; Davis et al., 2010). However, because both the BNST and amygdala consist of multiple interconnected subnuclei, the relationship between nuclei in this network could be quite complicated. Other brain structures, such as the parabrachial nucleus, which receives input from the BNST, may also play a role (Kaur et al., 2013). Future studies will be necessary to further characterize these complex circuits.

Freezing is thought to represent an important defensive response to threat. For example, in a predator–prey confrontation, freezing probably serves the prey by helping to avoid detection. The finding that BNST lesions not only reduced CO_2-evoked freezing, but also reduced conditioned place avoidance to CO_2 is consistent with BNST-dependent responses as expression of negative emotion. However, it is not yet clear why freezing might be an adaptive in circumstances associated with rising levels of CO_2. Perhaps when CO_2 is high or pH is low, movement is risky from a cardiorespiratory standpoint. Or perhaps freezing is an orienting response to further assess any type of threat. Furthermore, under some conditions, freezing might be counteradaptive by slowing escape from dangerously high CO_2 levels. It remains uncertain what CO_2-evoked freezing behavior represents or how it might be related to the anxiety, fear, and panic evoked by CO_2 in humans.

Nevertheless, our mouse studies suggest that the BNST might be important for CO_2-evoked responses in humans and that ASICs may be critical. Our data raise the possibility that elevated ASIC1A expression or function in the BNST might exaggerate CO_2-triggered responses in humans, thus suggesting a theoretically plausible mechanism for increased CO_2 sensitivity in panic disorder patients. Similarly, our results suggest that the BNST might be a critical extra-amygdalar structure underlying elevated CO_2 responses in humans with amygdala lesions (Feinstein et al., 2013; Smoller et al., 2014). Conversely, our results suggest that reducing ASIC1A expression or function in the BNST may reduce CO_2 responses and that ASIC1A antagonists might have therapeutic potential for anxiety disorders, especially those accompanied by CO_2 hypersensitivity.

References

Alvarez RP, Chen G, Bodurka J, Kaplan R, Grillon C (2011) Phasic and sustained fear in humans elicits distinct patterns of brain activity. Neuroimage 55:389–400. CrossRef Medline

Avery SN, Clauss JA, Winder DG, Woodward N, Heckers S, Blackford JU (2014) BNST neurocircuitry in humans. Neuroimage 91:311–323. CrossRef Medline

Brannan S, Liotti M, Egan G, Shade R, Madden L, Robillard R, Abplanalp B, Stofer K, Denton D, Fox PT (2001) Neuroimaging of cerebral activations and deactivations associated with hypercapnia and hunger for air. Proc Natl Acad Sci U S A 98:2029–2034. CrossRef Medline

Chandrashekar J, Yarmolinsky D, von Buchholtz L, Oka Y, Sly W, Ryba NJ, Zuker CS (2009) The taste of carbonation. Science 326:443–445. CrossRef Medline

Coryell MW, Ziemann AE, Westmoreland PJ, Haenfler JM, Kurjakovic Z, Zha XM, Price M, Schnizler MK, Wemmie JA (2007) Targeting ASIC1a reduces innate fear and alters neuronal activity in the fear circuit. Biol Psychiatry 62:1140–1148. CrossRef Medline

Coryell MW, Wunsch AM, Haenfler JM, Allen JE, McBride JL, Davidson BL, Wemmie JA (2008) Restoring acid-sensing ion channel-1a in the amygdala of knock-out mice rescues fear memory but not unconditioned fear responses. J Neurosci 28:13738–13741. CrossRef Medline

Coryell MW, Wunsch AM, Haenfler JM, Allen JE, Schnizler M, Ziemann AE, Cook MN, Dunning JP, Price MP, Rainier JD, Liu Z, Light AR, Langbehn DR, Wemmie JA (2009) Acid-sensing ion channel-1a in the amygdala, a novel therapeutic target in depression-related behavior. J Neurosci 29:5381–5388. CrossRef Medline

Cummins EP, Selfridge AC, Sporn PH, Sznajder JI, Taylor CT (2014) Carbon dioxide-sensing in organisms and its implications for human disease. Cell Mol Life Sci 71:831–845. CrossRef Medline

Davis M (2002) Neural circuitry of anxiety and stress disorders. In: Neuropsychopharmacology: the fifth generation of progress (Davis KL, Coyle JT, Nemeroff C, eds), pp 931–951. Philadelphia: Lippincott, Williams and Wilkins.

Davis M, Walker DL, Miles L, Grillon C (2010) Phasic vs sustained fear in rats and humans: role of the extended amygdala in fear vs anxiety. Neuropsychopharmacology 35:105–135. CrossRef Medline

Esquivel G, Schruers K, Griez E (2008) Experimental models: panic and fear. In: Handbook of anxiety and fear (Blanchard RJ, Griebel G, Nutt D, ed), pp 413–434. New York: Elsevier.

Evans KC, Banzett RB, Adams L, McKay L, Frackowiak RS, Corfield DR (2002) BOLD fMRI identifies limbic, paralimbic, and cerebellar activation during air hunger. J Neurophysiol 88:1500–1511. Medline

Feinstein JS, Buzza C, Hurlemann R, Follmer RL, Dahdaleh NS, Coryell WH, Welsh MJ, Tranel D, Wemmie JA (2013) Fear and panic in humans with bilateral amygdala damage. Nat Neurosci 16:270–272. CrossRef Medline

Fendt M, Endres T, Apfelbach R (2003) Temporary inactivation of the bed nucleus of the stria terminalis but not of the amygdala blocks freezing induced by trimethylthiazoline, a component of fox feces. J Neurosci 23:23–28. Medline

Flume PA, Eldridge FL, Edwards LJ, Mattison LE (1996) Relief of the 'air hunger' of breathholding: a role for pulmonary stretch receptors. Respir Physiol 103:221–232. CrossRef Medline

Gorman JM, Kent JM, Sullivan GM, Coplan JD (2000) Neuroanatomical hypothesis of panic disorder, revised. Am J Psychiatry 157:493–505. CrossRef Medline

Gregersen N, Dahl HA, Buttenschøn HN, Nyegaard M, Hedemand A, Als TD, Wang AG, Joensen S, Woldbye DP, Koefoed P, Kristensen AS, Kruse TA, Børglum AD, Mors O (2012) A genome-wide study of panic disorder suggests the amiloride-sensitive cation channel 1 as a candidate gene. Eur J Hum Genet 20:84–90. CrossRef Medline

Grupe DW, Oathes DJ, Nitschke JB (2013) Dissecting the anticipation of aversion reveals dissociable neural networks. Cereb Cortex 23:1874–1883. CrossRef Medline

Haufler D, Nagy FZ, Pare D (2013) Neuronal correlates of fear conditioning

in the bed nucleus of the stria terminalis. Learn Mem 20:633–641. CrossRef Medline

Hodges MR, Tattersall GJ, Harris MB, McEvoy SD, Richerson DN, Deneris ES, Johnson RL, Chen ZF, Richerson GB (2008) Defects in breathing and thermoregulation in mice with near-complete absence of central serotonin neurons. J Neurosci 28:2495–2505. CrossRef Medline

Hruska-Hageman AM, Benson CJ, Leonard AS, Price MP, Welsh MJ (2004) PSD-95 and Lin-7b interact with acid-sensing ion channel-3 and have opposite effects on H^+-gated current. J Biol Chem 279:46962–46968. CrossRef Medline

Hu J, Zhong C, Ding C, Chi Q, Walz A, Mombaerts P, Matsunami H, Luo M (2007) Detection of near-atmospheric concentrations of CO_2 by an olfactory subsystem in the mouse. Science 317:953–957. CrossRef Medline

Kaur S, Pedersen NP, Yokota S, Hur EE, Fuller PM, Lazarus M, Chamberlin NL, Saper CB (2013) Glutamatergic signaling from the parabrachial nucleus plays a critical role in hypercapnic arousal. J Neurosci 33:7627–7640. CrossRef Medline

Kim SY, Adhikari A, Lee SY, Marshel JH, Kim CK, Mallory CS, Lo M, Pak S, Mattis J, Lim BK, Malenka RC, Warden MR, Neve R, Tye KM, Deisseroth K (2013) Diverging neural pathways assemble a behavioural state from separable features in anxiety. Nature 496:219–223. CrossRef Medline

Klein DF (1993) False suffocation alarms, spontaneous panics, and related conditions: an integrative hypothesis. Arch Gen Psychiatry 50:306–317. CrossRef Medline

Lang PJ, Wangelin BC, Bradley MM, Versace F, Davenport PW, Costa VD (2011) Threat of suffocation and defensive reflex activation. Psychophysiology 48:393–396. CrossRef Medline

LeDoux JE, Iwata J, Cicchetti P, Reis DJ (1988) Different projections of the central amygdaloid nucleus mediate autonomic and behavioral correlates of conditioned fear. J Neurosci 8:2517–2529. Medline

Lee Y, Davis M (1997) Role of the hippocampus, the bed nucleus of the stria terminalis, and the amygdala in the excitatory effect of corticotropin-releasing hormone on the acoustic startle reflex. J Neurosci 17:6434–6446. Medline

Liotti M, Brannan S, Egan G, Shade R, Madden L, Abplanalp B, Robillard R, Lancaster J, Zamarripa FE, Fox PT, Denton D (2001) Brain responses associated with consciousness of breathlessness (air hunger). Proc Natl Acad Sci U S A 98:2035–2040. CrossRef Medline

Luyten L, van Kuyck K, Vansteenwegen D, Nuttin B (2011) Electrolytic lesions of the bed nucleus of the stria terminalis disrupt freezing and startle potentiation in a conditioned context. Behav Brain Res 222:357–362. CrossRef Medline

Martínez-Lorenzana G, Jiménez JR, Condés-Lara M (2004) Interamygdaloid connection of basolateral nucleus through the anterior commissure in the rat. Neurosci Lett 366:154–157. CrossRef Medline

Mayhan WG, Faraci FM, Heistad DD (1988) Effects of vasodilatation and acidosis on the blood–brain barrier. Microvasc Res 35:179–192. CrossRef Medline

Mitchell RA, Carman CT, Severinghaus JW, Richardson BW, Singer MM, Shnider S (1965) Stability of cerebrospinal fluid pH in chronic acid-base disturbances in blood. J Appl Physiol 20:443–452. Medline

Paxinos G, Franklin KBJ (2001) The mouse brain in stereotaxic coordinates, Ed 2. San Diego: Academic.

Phelps EA, LeDoux JE (2005) Contributions of the amygdala to emotion processing: from animal models to human behavior. Neuron 48:175–187. CrossRef Medline

Pidoplichko VI, Aroniadou-Anderjaska V, Prager EM, Figueiredo TH, Almeida-Suhett CP, Miller SL, Braga MF (2014) ASIC1a activation enhances inhibition in the basolateral amygdala and reduces anxiety. J Neurosci 34:3130–3141. CrossRef Medline

Price MP, Gong H, Parsons MG, Kundert JR, Reznikov LR, Bernardinelli L, Chaloner K, Buchanan GF, Wemmie JA, Richerson GB, Cassell MD, Welsh MJ (2014) Localization and behaviors in null mice suggest that ASIC1 and ASIC2 modulate responses to aversive stimuli. Genes Brain Behav 13:179–194. CrossRef Medline

Rassovsky Y, Kushner MG (2003) Carbon dioxide in the study of panic disorder: issues of definition, methodology, and outcome. J Anxiety Disord 17:1–32. CrossRef Medline

Smoller JW, Gallagher PJ, Duncan LE, McGrath LM, Haddad SA, Holmes AJ, Wolf AB, Hilker S, Block SR, Weill S, Young S, Choi, EY, Rosenbaum JF, Biederman J, Faraone SV, Roffman JL, Manfro GG, Blaya C, Hirshfeld-Becker DR, Stein MB, et al. (2014) The human ortholog of acid-sensing ion channel gene ASIC1a is associated with panic disorder and amygdala structure and function. Biol Psychiatry. Advance online publication. Retrieved Jan. 18, 2014. doi: 10.1016/j.biopsych.2013.12.018. CrossRef Medline

Somerville LH, Whalen PJ, Kelley WM (2010) Human bed nucleus of the stria terminalis indexes hypervigilant threat monitoring. Biol Psychiatry 68:416–424. CrossRef Medline

Somerville LH, Wagner DD, Wig GS, Moran JM, Whalen PJ, Kelley WM (2013) Interactions between transient and sustained neural signals support the generation and regulation of anxious emotion. Cereb Cortex 23:49–60. CrossRef Medline

Sullivan GM, Apergis J, Bush DE, Johnson LR, Hou M, Ledoux JE (2004) Lesions in the bed nucleus of the stria terminalis disrupt corticosterone and freezing responses elicited by a contextual but not by a specific cue-conditioned fear stimulus. Neuroscience 128:7–14. CrossRef Medline

Waldmann R, Champigny G, Bassilana F, Heurteaux C, Lazdunski M (1997) A proton-gated cation channel involved in acid-sensing. Nature 386:173–177. CrossRef Medline

Walker DL, Davis M (2008) Role of the extended amygdala in short-duration versus sustained fear: a tribute to Dr. Lennart Heimer. Brain Struct Funct 213:29–42. CrossRef Medline

Wemmie JA, Chen J, Askwith CC, Hruska-Hageman AM, Price MP, Nolan BC, Yoder PG, Lamani E, Hoshi T, Freeman JH Jr, Welsh MJ (2002) The acid-activated ion channel ASIC contributes to synaptic plasticity, learning, and memory. Neuron 34:463–477. CrossRef Medline

Wemmie JA, Askwith CC, Lamani E, Cassell MD, Freeman JH Jr, Welsh MJ (2003) Acid-sensing ion channel 1 is localized in brain regions with high synaptic density and contributes to fear conditioning. J Neurosci 23:5496–5502. Medline

Wemmie JA, Taugher RJ, Kreple CJ (2013) Acid-sensing ion channels in pain and disease. Nat Rev Neurosci 14:461–471. CrossRef Medline

Zha XM, Wemmie JA, Green SH, Welsh MJ (2006) Acid-sensing ion channel 1a is a postsynaptic proton receptor that affects the density of dendritic spines. Proc Natl Acad Sci U S A 103:16556–16561. CrossRef Medline

Zha XM, Costa V, Harding AM, Reznikov L, Benson CJ, Welsh MJ (2009) ASIC2 subunits target acid-sensing ion channels to the synapse via an association with PSD-95. J Neurosci 29:8438–8446. CrossRef Medline

Ziemann AE, Allen JE, Dahdaleh NS, Drebot II, Coryell MW, Wunsch AM, Lynch CM, Faraci FM, Howard MA 3rd, Welsh MJ, Wemmie JA (2009) The amygdala is a chemosensor that detects carbon dioxide and acidosis to elicit fear behavior. Cell 139:1012–1021. CrossRef Medline